Dalton Transactions

Cite this: *Dalton Trans.*, 2011, **40**, 2451

www.rsc.org/dalton

PAPER

Dansyl-anthracene dyads for ratiometric fluorescence recognition of Cu^{2+}†

Kuljit Kaur and Subodh Kumar*

Received 15th August 2010, Accepted 13th December 2010
DOI: 10.1039/c0dt01016b

Dansyl-anthracene dyads **1** and **2** in CH_3CN–H_2O (7 : 3) selectively recognize Cu^{2+} ions amongst alkali, alkaline earth and other heavy metal ions using both absorbance and fluorescence spectroscopy. In absorbance, the addition of Cu^{2+} to the solution of dyads **1** or **2** results in appearance of broad absorption band from 200 nm to 725 nm for dyad **1** and from 200 nm to 520 nm for dyad **2**. This is associated with color change from colorless to blue (for **1**) and fluorescent green (for **2**). This bathochromic shift of the spectrum could be assigned to internal charge transfer from sulfonamide nitrogen to anthracene moiety. In fluorescence, under similar conditions dyads **1** and **2** on addition of Cu^{2+} selectively quench fluorescence due to dansyl moiety between 520–570 nm (for **1**)/555–650 nm (for **2**) with simultaneous fluorescence enhancement at 470 nm and 505 nm for dyads **1** and **2**, respectively. Hence these dyads provide opportunity for ratiometric analysis of 1–50 μM Cu^{2+}. The other metal ions *viz*. Fe^{3+}, Co^{2+}, Ni^{2+}, Cd^{2+}, Zn^{2+}, Hg^{2+}, Ag^{+}, Pb^{2+}, Li^{+}, Na^{+}, K^{+}, Mg^{2+}, Ca^{2+}, Ba^{2+} do not interfere in the estimation of Cu^{2+} except Cr^{3+} in case of dyad **1**. The coordination of dimethylamino group of dansyl unit with Cu^{2+} causes quenching of fluorescence due to dansyl moiety between 520–600 nm and also restricts the photoinduced electron transfer from dimethylamino to anthracene moiety to release fluorescence between 450–510 nm. This simultaneous quenching and release of fluorescence respectively due to dansyl and anthracene moieties emulates into Cu^{2+} induced ratiometric change.

Introduction

The development of chemosensors for heavy metal ions[1] is a demanding area of research due to their biological and environmental relevance. Fluorescent sensors[2] for cations are especially attractive due to their high sensitivity and simple detection methods.

Because copper is an essential trace element in biological systems at low concentration but acts as a pollutant when its concentration is high, as it can cause oxidative stress and disorders associated with neurodegenerative diseases such as Alzheimer's disease,[3] there is particular attention on the design of new fluorescent probes for the detection of copper ion.[4] However, many of the reported Cu^{2+} fluorescent chemosensors undergo fluorescence quenching[5] upon the addition of Cu^{2+}, although there are some probes that show fluorescence enhancement.[6] Compared to fluorescence quenching and enhancement, a ratiometric fluorescent response due to ON-OFF-ON process at two different acquisition wavelengths provides advantage over ON-OFF and OFF-ON based chemosensors and is considered to be more efficient, not only because of its higher sensitivity but also because of its better resistance to background fluorescence and variation of fluorescent probe concentration. Further rationing of the signal allows single reading based evaluation of species concentration. In particular, development of ratiometric probes for Cu^{2+} ions[7] is a challenge due to its inherent paramagnetic nature and hence complexation generally results in quenching of fluorescence intensity of the probe.

In case of dual fluorophore-based chemosensors, the communication between two fluorophores present in a single molecular probe can be decreased or increased by the presence of an analyte. This is evident by the simultaneous decrease and increase in intensity of the two fluorophore moieties in the presence of analyte. This situation not only increases the sensitivity of the molecular system towards an analyte but also provides opportunities for ratiometric analysis of the analyte. Such communication between two fluorophores could be miniaturized through different mechanisms, *viz*. Fluorescence Resonance Energy Transfer (FRET) between two fluorophores, Photoinduced Electron Transfer (PET) mechanism or through Internal Charge Transfer (ICT) mechanism. The FRET has been quite commonly used for devising dyads for Cu^{2+}, Zn^{2+}, Hg^{2+}, Pb^{2+} and Cr^{3+}.[8]

In design of such fluorescence-based probes, the selection of fluorophore plays a significant role in selectivity and sensitivity of the molecular sensor. Amongst commonly used fluorescent moieties like naphthalene[7d,9] anthracene, pyrene,[7f,7i] quinoline, benzimidazole, dansyl, naphthalimide,[7e,7k] *etc.*, the dansyl group has been quite generously used because of its characteristic spectroscopic properties like absorbance in near UV-region, fluorescence band in visible region with relatively large Stokes shift,

Department of Chemistry, Guru Nanak Dev University, Amritsar, India. E-mail: subodh_gndu@yahoo.co.in

† Electronic supplementary information (ESI) available. See DOI: 10.1039/c0dt01016b

sensitivity of emission spectrum to chemical environment and is also the smallest available fluorophore. Dansyl has been commonly used as a fluorescent tag with biomolecules like proteins, lipids, peptides, DNA, *etc.* for understanding molecular interactions. In recent years, the dansyl-based synthetic probes[10] have gained attention for designing molecular probes for anions and cations. Fluorescent chemosensors based on calixarene scaffold utilizing dansyl as fluorescent tag have found use for detection of various metal ions like Pb^{2+}, Hg^{2+}, Cu^{2+} *etc.*, but small molecular probes are well suited for quick detection of various metal ions and for *in vivo* studies in biological systems.

Conspicuously, dansyl amide of alkyl amine[8b] or *p*-toluenesulfonamide of fluorescent pyrenemethylamine,[7i] even in the absence of any other coordination site, have been found to form 1 : 2 complexes selectively with Cu^{2+}. In the case of *p*-toluenesulfonamide of pyrenemethylamine, the selective static fluorescence due to excimer formation between pyrenyl groups of two chemosensor molecules enables ratiometric estimation of Cu^{2+}.

In the present work, we have synthesized two new dyads **1** and **2** based on dansyl and anthracene fluorophores and three model compounds **3–5** for comparison and have investigated their photophysical behavior towards various monovalent and divalent metal ions. The dyads **1** and **2** bind selectively with Cu^{2+} ions as compared to other metal ions and signal the binding event through simultaneous increase in fluorescence between 450–500 nm and decrease in fluorescence between 515–600 nm. This simultaneous increase and decrease at two acquisition wavelengths could be used for ratiometric detection of Cu^{2+} and indicates their potential use as sensitive fluorescence ratiometric probes for the selective recognition of Cu^{2+} ions. The poor response of model compounds **3–5**, lacking either dansyl or the anthracene unit, towards Cu^{2+} and other metal ions under the conditions studied here further highlights the significance of dyad structural architect in probes **1** and **2** for ratiometric analysis of Cu^{2+}.

Results and discussion

Synthesis of dyads 1–5

The probes **1–5** have been synthesized by stirring the solution of respective 1-anthracenamine (**7**)/2-anthracenamine (**8**)/aniline (**9**) and triethylamine in dichloromethane with dansyl chloride (**6**)/*p*-toluenesulfonyl chloride (**10**) at room temperature (Scheme 1). The structures of the probes were characterized by ^1H - ^1H decoupling, ^{13}C NMR, HRMS and elemental analysis.

UV-Vis absorption studies of dyads 1–5

Dyad **1** (25 μM, CH_3CN–H_2O (7 : 3), HEPES buffer pH 7.0 ± 0.1) displayed an absorption spectrum with a structured band having λ_{max} at 365 nm (ε = 8800 l mol^{-1} cm^{-1}), 345 nm (ε = 9200 l mol^{-1} cm^{-1}) and 385 nm (ε = 7000 l mol^{-1} cm^{-1}). On addition of different metal ions, *viz*. Li^+, Na^+, K^+, Mg^{2+}, Ca^{2+}, Ba^{2+}, Cr^{3+}, Fe^{2+}, Co^{2+}, Ni^{2+}, Zn^{2+}, Hg^{2+}, Cd^{2+}, Ag^+ and Pb^{2+}, to solution of **1**, there is no significant change in its UV-vis spectrum except in case of addition of Cu^{2+} ions. On addition of Cu^{2+} to the solution of **1**, a new broad absorption band with absorption in the range of 400–725 nm appeared (Fig. 1). The appearance

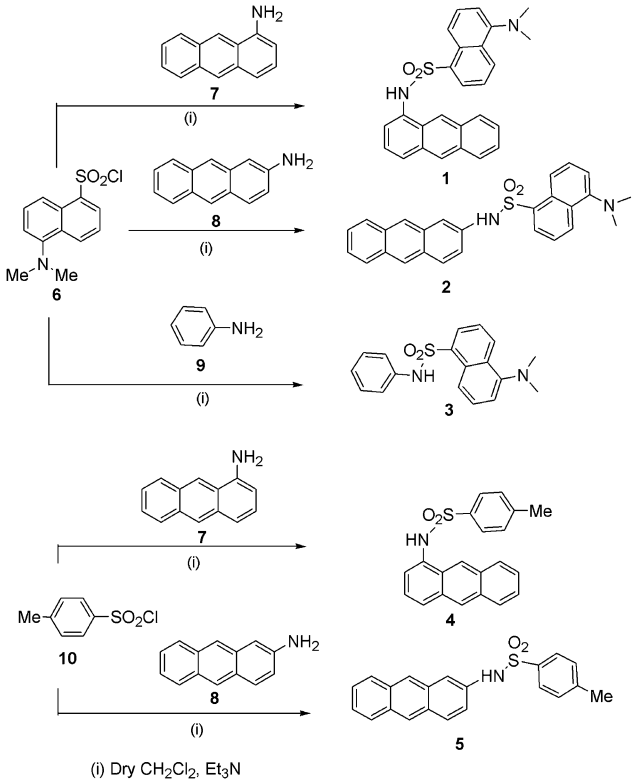

Scheme 1 Synthesis of dyads **1–5**.

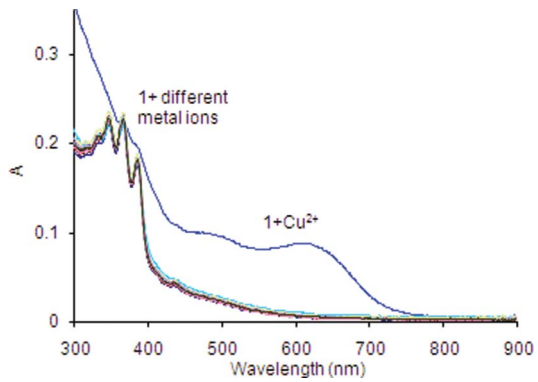

Fig. 1 Effect of addition of different metal ions on the UV-vis. spectrum of dyad **1** (25 μM, CH_3CN : H_2O (7 : 3), HEPES (0.01 M), pH 7.0 ± 0.1) [Different metal ions are Cr^{3+}, Fe^{3+}, Co^{2+}, Ni^{2+}, Cu^{2+}, Cd^{2+}, Zn^{2+}, Hg^{2+}, Ag^+, Pb^{2+}, Li^+, Na^+, K^+, Mg^{2+}, Ca^{2+}, Ba^{2+}].

of broad range absorption band is associated with change in color of the solution from colorless to blue and points to the deprotonation of sulfonamide NH and delocalization of negative charge on both sulfonamide and anthracene moieties. Therefore, probe **1** shows selective complexation towards Cu^{2+} with unique absorption behavior. The spectral fitting of the absorption data obtained by titration of **1** with Cu^{2+} (Fig. 2) shows the formation of 1 : 1 stoichiometric **1**-Cu^{2+} complex ($\log\beta$ = 5.1 ± 0.1) with lowest detection limit of Cu^{2+} 2.5 μM.

Similarly, dyad **2** (25 μM, CH_3CN–H_2O (7 : 3), HEPES buffer pH 7.0 ± 0.1), having dansyl group placed at position **2** of anthracenamine moiety, displayed an absorption spectrum (Fig. 3) with a structured band having λ_{max} at 338 nm (ε = 13 284 l mol^{-1} cm^{-1})

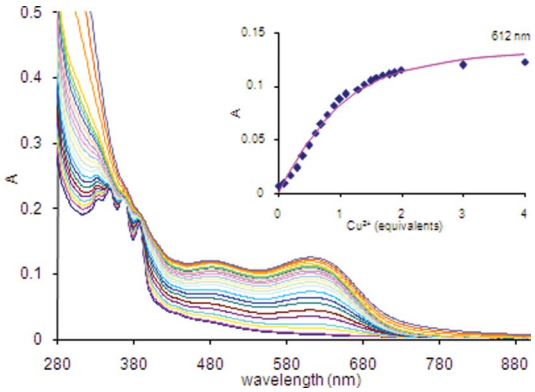

Fig. 2 Effect of gradual addition of Cu^{2+} ions on the UV-vis. spectrum of dyad **1** (25 μM, CH_3CN : H_2O (7 : 3), HEPES (0.01 M), pH 7.0 ± 0.1). The inset shows the increase in absorbance at 612 nm on gradual addition of Cu^{2+} ions to the solution of **1**. The points refer to experimental values and line shows the spectral fit.

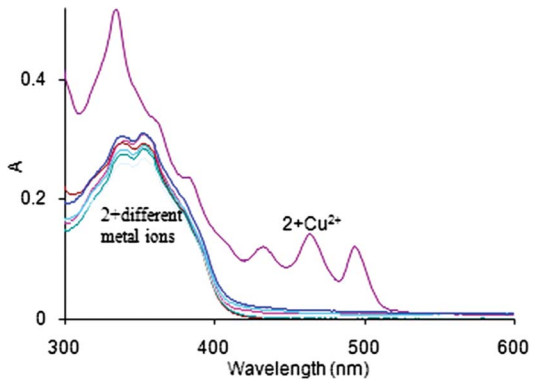

Fig. 3 Effect of addition of different metal ions on the UV-vis. spectrum of dyad **2** (25 μM, CH_3CN : H_2O (7 : 3), HEPES (0.01 M) pH 7.0 ± 0.1) [Different metal ions are Cr^{3+}, Fe^{3+}, Co^{2+}, Ni^{2+}, Cu^{2+}, Cd^{2+}, Zn^{2+}, Hg^{2+}, Ag^{+}, Pb^{2+}, Li^{+}, Na^{+}, K^{+}, Mg^{2+}, Ca^{2+}, Ba^{2+}].

and 352 nm ($\varepsilon = 13\,328\ l\ mol^{-1}\ cm^{-1}$). On addition of different metal ions to the solution of **2**, only addition of Cu^{2+} ions caused the formation of a red shifted structured absorption band with λ_{max} at 432 nm, 464 nm and 494 nm associated with change in color of the solution from colorless to fluorescent green. The spectral fitting of the absorption data obtained by titration of **2** with Cu^{2+} (Fig. 4) shows the formation of 1 : 1 stoichiometric complex with $\log \beta = 4.03 \pm 0.1$ with lowest detection limit of 10 μM. The lower red shift of absorption band on addition of Cu^{2+} to dyad **2** than that observed in case of dyad **1** shows the significance of position of dansyl amide moiety at anthracene moiety in its sensitivity to metal ions.

The addition of Cu^{2+} ions to the solution of dyads **1** and **2** in pure CH_3CN showed significantly lower absorption changes (Fig. S1 and S2, ESI†) as compared to that observed in CH_3CN–H_2O (7 : 3) mixture. The spectral fitting of the titration data shows the formation of relatively weaker complex ($\log \beta = 3.72 \pm 0.2$) of **1** with Cu^{2+} in pure acetonitrile than that observed in CH_3CN–H_2O ($\log \beta = 5.1 \pm 0.1$). This points to the deprotonation of dyads **1** and **2** in presence of Cu^{2+} and formation of ionic complexes of these dyads with Cu^{2+} in aqueous medium. The presence of water is essential for appearance of blue or green colors on addition of Cu^{2+} to dyads **1** and **2**. The deprotonation of the probes

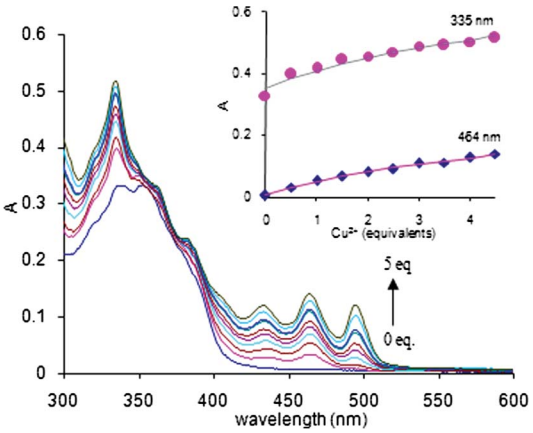

Fig. 4 Effect of gradual addition of Cu^{2+} ions on the UV-vis. spectrum of dyad **2** (25 μM, CH_3CN : H_2O (7 : 3), HEPES (0.01 M) pH 7.0 ± 0.1). The inset shows the increase in absorbance at 335 nm and 464 nm on gradual addition of Cu^{2+} ions to the solution of **2**. The points refer to experimental values and line shows the spectral fit.

1 and **2** on interaction with Cu^{2+} has been further confirmed by analysing pH induced changes in absorbance behaviour of probes **1** and **2** and their Cu^{2+} complexes through spectral fitting. These titration data show that probes **1** and **2**, between pH 4–9 remain as neutral molecule but at pH < 4 undergo protonation at dimethylamino group to form monocation species and at pH > 9, undergo deprotonation at sulfonamide group to give monoanion species (Fig. S3, ESI†). However, 1 : 1 **1**-Cu^{2+} solution between pH 6.5–8.5 remains as **1**(anion)-Cu^{2+} complex which at higher pH is converted to hydroxide complex [1(anion)-Cu^{2+} (OH^-)] and at lower pH values is converted to **1**-Cu^{2+} complex (Fig. S4 and S5†). Similar trend is shown by dyad **2**. Therefore, dyads **1** and **2** which exist as neutral molecule at pH 7, on addition of Cu^{2+} ions undergo deprotonation to form **1**/**2**(anion)-Cu^{2+} complex.

The dansyl amide of aniline, *i.e.* probe **3** (25 μM, CH_3CN–H_2O (7 : 3), HEPES buffer pH 7.0 + 0.1), on addition of Cu^{2+} (Fig. S6, ESI†) and other metal ions did not show any discernible spectral or color change and highlights the significance of anthracene moiety in dyads **1** and **2** in the recognition of Cu^{2+}.

The appearance of similar UV-vis. spectra in case of **1** + Cu^{2+} and **4** + Cu^{2+} solutions and that of **2** + Cu^{2+} and **5** + Cu^{2+} solutions in CH_3CN: H_2O (7 : 3), HEPES 0.01 M, pH 7.0 (Fig. 5) points

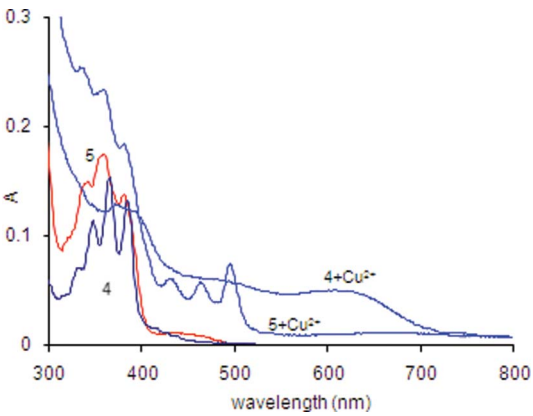

Fig. 5 Effect of addition of Cu^{2+} on the UV-vis. spectra of probes **4** and **5** (25 μM, CH_3CN : H_2O (7 : 3), HEPES 0.01 M, pH 7.0 ± 0.1).

that in the ground state these molecules interact with Cu^{2+} in a similar manner. The similar association constants for coordination of Cu^{2+} with probes **4** ($\log\beta = 4.8 \pm 0.1$) and **5** ($\log\beta = 4.0 \pm 0.1$) with that of dyads **1** ($(\log\beta = 5.1 \pm 0.1)$ and dyad **2** ($\log\beta = 4.03 \pm 0.1$) clearly point the dansyl or *p*-toluene moieties have insignificant effect in absorbance based estimation of Cu^{2+}.

Fluorescence studies of dyads 1–5

Dyad **1** (2 μM, CH_3CN, $\Phi = 0.033$), on excitation at 335 nm, displayed emission bands at 440 nm, 470 nm (anthracene moiety) and 516 nm (typical of dansyl moiety) which underwent fluorescence quenching on addition of Cu^{2+} (Fig. 6). Therefore on excitation at 335 nm both anthracene and dansyl moieties are excited and exhibit respective fluorescence bands. The spectral fitting of the titration data of dyad **1** (2 μM, CH_3CN) with Cu^{2+} shows the formation of ML ($\log\beta = 9.6 \pm 0.2$), M_2L ($\log\beta = 17.9 \pm 0.3$) and M_3L ($\log\beta = 23.4 \pm 0.3$) species. The careful examination of the fluorescence quenching on addition of Cu^{2+} ions to the solution of **1** shows that emission intensity due to dansyl moiety at 516 nm is quenched by >90% on addition of 5 μM Cu^{2+} ions, whereas the complete quenching of fluorescence due to anthracene moiety is delayed to the addition of 10 μM Cu^{2+} ions. Therefore, anthracene and dansyl moieties in CH_3CN solution of dyad **1** respond to Cu^{2+} in a different manner.

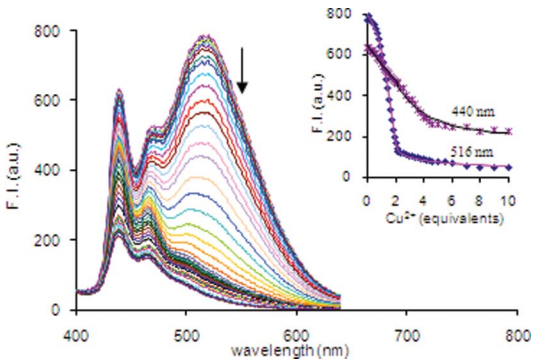

Fig. 6 Effect of gradual addition of Cu^{2+} ions on the fluorescence spectrum of dyad **1** (2 μM, CH_3CN). Inset shows the spectral fitting of the titration curve (λ_{ex} 335 nm).

Dyad **1** (1 μM, $CH_3CN : H_2O$ (7 : 3), HEPES 0.1 mM, pH 7.0 ± 0.1, $\Phi = 0.026$), on addition of different alkali, alkaline earth and heavy metal ions, *viz*. Cr^{3+}, Fe^{2+}, Co^{2+}, Ni^{2+}, Zn^{2+}, Hg^{2+}, Cd^{2+}, Ag^{+} and Pb^{2+}, displayed no significant change in the emission spectrum (Fig. 7) except on addition of Cu^{2+}. On gradual addition of Cu^{2+} ions, the fluorescence spectrum of dyad **1** (Fig. 8a) showed gradual quenching of emission band at 515 nm with a small hypsochromic shift which is associated with concomitant increase in fluorescence intensity at 470 nm. The spectral fitting of the data shows the formation of ML ($\log\beta = 7.0 \pm 0.3$), M_2L ($\log\beta = 12.0 \pm 0.6$) and M_3L ($\log\beta = 18.2 \pm 0.3$) stoichiometric species.

The decrease in $\log\beta$ values in CH_3CN–H_2O mixture in comparison to that observed in pure CH_3CN is in general agreement with the lower complexation due to higher solvation of metal ions and ligand sites in presence of water. The simultaneous decrease and increase in emission intensity respectively at 560 nm and 470 nm, arising on addition of Cu^{2+} to aqueous solution of dyad **1** provides opportunities for elaboration of ratiometric approach for

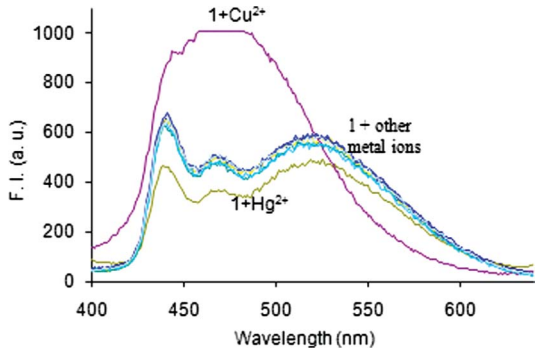

Fig. 7 Effect of different metal ions on the fluorescence spectrum of dyad **1** (3 μM, $CH_3CN : H_2O$ (7 : 3), HEPES 0.01 M, pH 7.0 ± 0.1. (λ_{ex} : 335 nm).

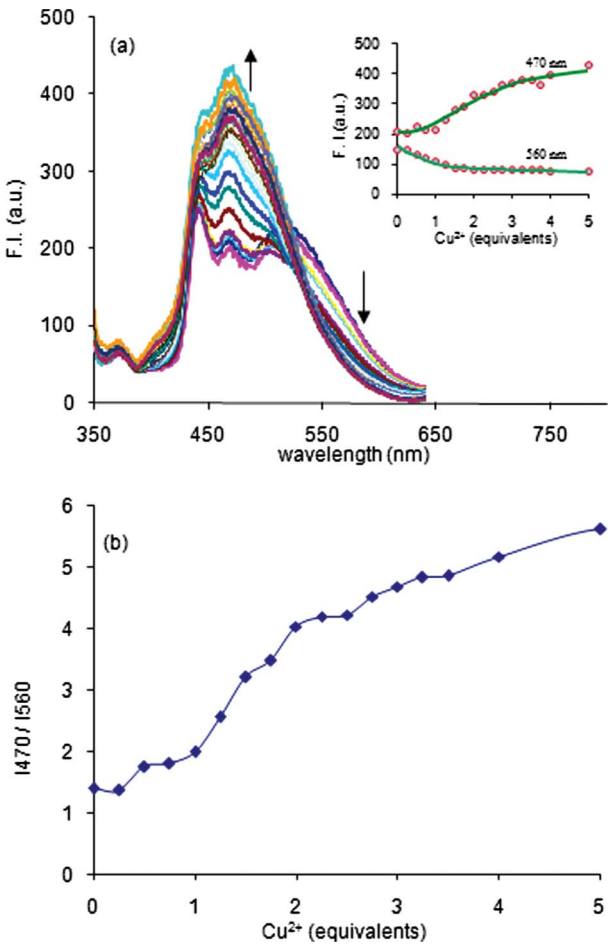

Fig. 8 (a) Effect of different concentrations of Cu^{2+} on emission spectrum of **1** (1 μM, CH_3CN: H_2O (7 : 3) HEPES buffer, 0.01 M, pH 7. (b) Fluorescence ratiometric response (I_{470}/I_{560}) of **1** (1 μM) on addition of Cu^{2+} ions (λ_{ex} : 335 nm).

the estimation of Cu^{2+} using rationing of fluorescence intensities at I_{470}/I_{560} for sensing of 0.5–5 μM Cu^{2+} (Fig. 8b).

The bar graph between ratio of emission intensities at 470 nm and 560 nm *versus* different metal ions (Fig. S7, ESI†) shows the selective recognition of Cu^{2+}. To check the practical applicability of dyad **1** as Cu^{2+} selective fluorescent probe, competition experiments were performed. The addition of different metal ions, *viz*. Ni^{2+}, Hg^{2+}, Co^{2+}, Cd^{2+}, Ag^{+}, Zn^{2+} (50 μM), to solution of

1 + Cu^{2+} (5 μM) did not affect the ratio of emission intensity obtained for **1**+Cu^{2+} solution. The decrease in emission ratio of **1**+Cu^{2+} on addition of Cr^{3+} shows its interference in estimation of Cu^{2+} (Fig. S8, ESI†). Hence, **1** is acting as selective ratiometric probe for Cu^{2+}.

In case of dyad **2** (0.5 μM, CH_3CN), the gradual addition of Cu^{2+} ions caused gradual decrease in emission intensity at 544 nm with hypsochromic shift of the emission band to 475 nm (Fig. 9). The spectral fitting analysis of the titration data shows the formation of M_3L species ($\log \beta = 18.71 \pm 0.1$).

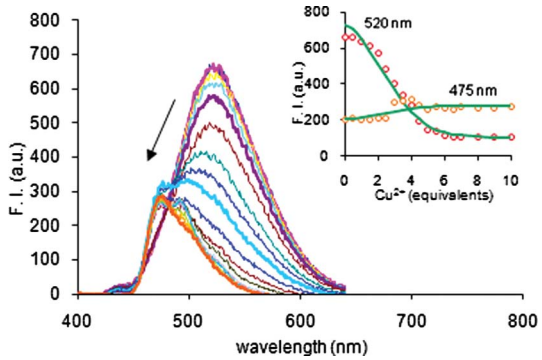

Fig. 9 Effect of gradual addition of Cu^{2+} on the fluorescence spectrum of dyad **2** (0.5 μM, CH_3CN, λ_{ex} 335 nm). Inset shows the spectral fitting of the titration curve at 520 and 475 nm.

Dyad **2** (1 μM, CH_3CN : H_2O (7 : 3) HEPES 0.01 M, pH 7.0) on excitation at 375 nm, displayed an emission spectrum with λ_{em} at 544 nm. The addition of alkali, alkaline earth and heavy metal ions, *viz*. Cr^{3+}, Fe^{2+}, Co^{2+}, Ni^{2+}, Zn^{2+}, Hg^{2+}, Cd^{2+}, Ag^{+} and Pb^{2+}, displayed no significant change in the emission spectrum of dyad **2** (Fig. S9, ESI†). The gradual addition of Cu^{2+} to the solution of dyad **2**, caused decrease in emission intensity between 555–650 nm with concomitant increase in intensity at 505 nm (Fig. 10a). The spectral fitting of the data shows the formation of M_2L ($\log \beta = 12.17 \pm 0.4$) and M_3L ($\log \beta = 16.59 \pm 0.4$). This situation provides an opportunity of ratiometric sensing of Cu^{2+} in 1–40 μM range. (Fig. 10b). In this range, the increase in ratio of intensities shows linear increase.

The analysis of species distribution diagram for complexation of Cu^{2+} with dyad **2** both in absorbance and fluorescence based titrations shows that in the ground state only one Cu^{2+} ion binds with dyad **2** but in the excited state two more Cu^{2+} ions bind with dyad **2** resulting in formation of M_2L and M_3L species (Fig. 11). Both these species cause simultaneous decrease and increase in fluorescence respectively due to dansyl and anthracene moieties but this change is remarkably higher in case of M_3L than observed in case of M_2L.

The bar diagrams (Fig. 12) between ratio of emission intensities at 505 nm and 590 nm *versus* different metal ions and effect of presence of interfering metal ions show the selective recognition of Cu^{2+} and practical applicability of dyad **2** as ratiometric probe in the presence of other metal ions.

The solution of probe **3**, in CH_3CN : H_2O (7 : 3), HEPES 0.01 M, pH 7.0, on excitation at 335 nm gave λ_{em} at 525 nm typical of dansyl group but emission remains unaffected by the presence of metal ions even in large excess (Fig. S11, ESI†). Probes **4** and **5** in CH_3CN : H_2O (7 : 3), HEPES 0.01 M, pH 7.0, on

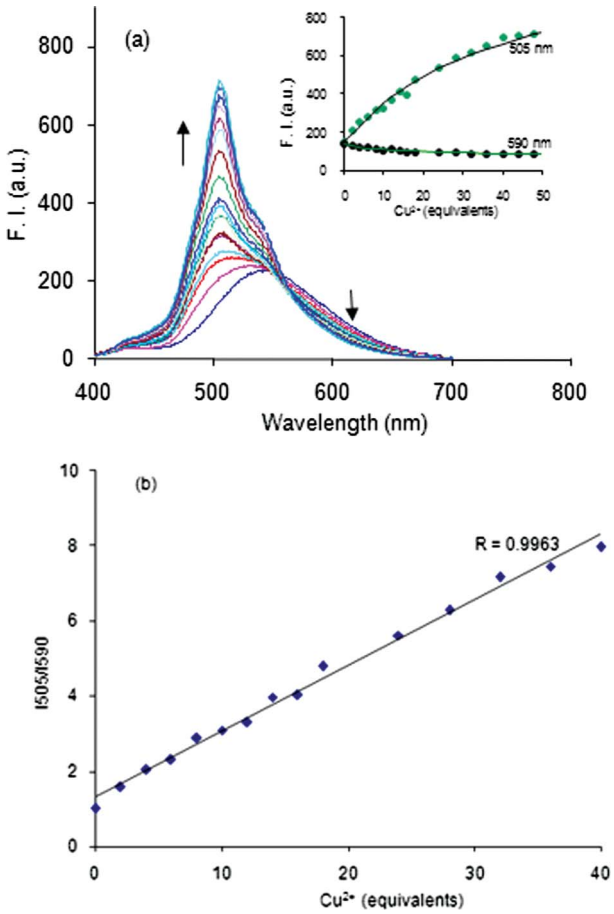

Fig. 10 (a) Effect of gradual addition of Cu^{2+} on emission spectrum of **2** (1 μM, CH_3CN: H_2O (7 : 3) HEPES buffer, 0.01 M, pH 7). Inset shows the spectral fitting of the titration curve at 505 nm and 590 nm. (b) Fluorescence ratiometric response (I_{505}/I_{590}) of **2** (1 μM) towards Cu^{2+} ions (λ_{ex}: 375 nm).

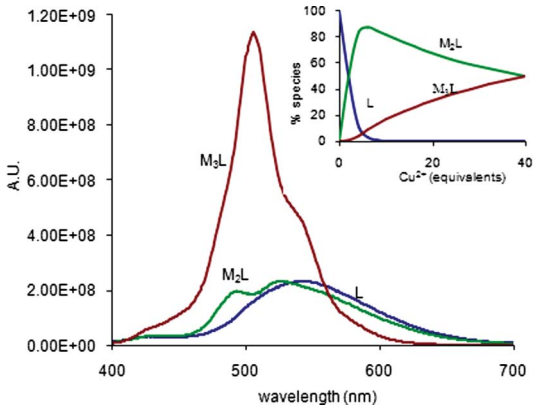

Fig. 11 Species distribution curve from fluorescence titration of dyad **2** with Cu^{2+}.

excitation at 335 nm gave λ_{em} at 425 nm typical of anthracene moiety. The solution of probe **4** on keeping for more than 3 h undergoes λ_{em} shift from 423 nm to 480 nm. Probably **4** undergoes aggregation under these conditions and λ_{em} arises due to excimer formation of anthracene moieties. The fluorescence of probes **4** and **5** remains unaffected by the addition of metal ions

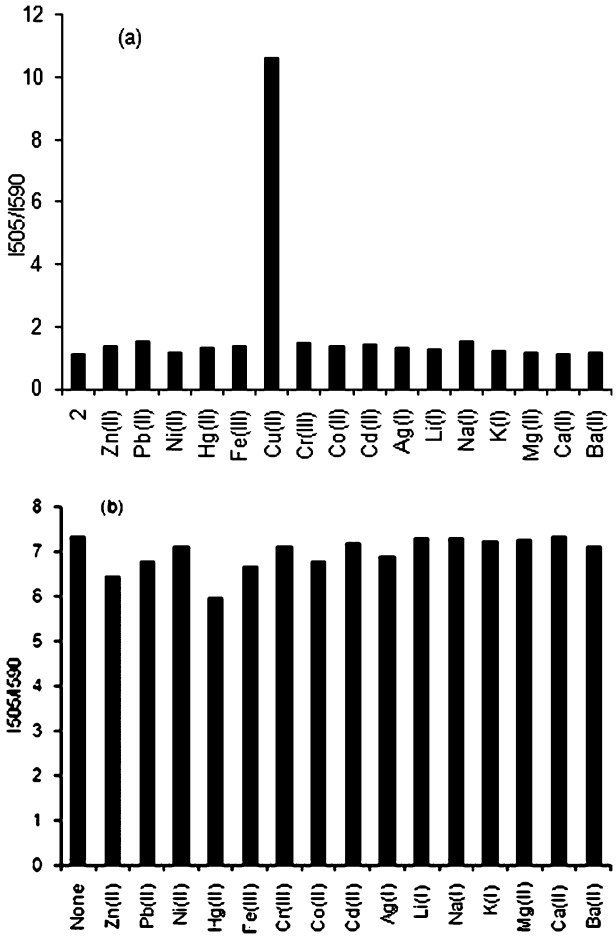

Fig. 12 : Fluorescence ratiometric response (I_{505}/I_{590}) of dyad **2** (1 μM, CH_3CN–H_2O (7 : 3) HEPES 0.01 M, pH 7.0 ± 0.1 (λ_{ex}: 375 nm)) (a) on addition of different metal ions (100 μM), (b) on addition of Cu^{2+} (50 μM) with different metal ions (100 μM).

including Cu^{2+} (Fig. S12, ESI†). These results unambiguously point to the role of communication between anthracene and dansyl fluorophores in dyads **1** and **2** responsible for characteristic ratiometric fluorescence changes arising on addition of Cu^{2+}.

Therefore, in the ground state dyads **1** and **2** complex with only one Cu^{2+} to cause bathochromically shifted UV-Vis spectrum. This change remains unaffected even when the dansyl moieties are replaced by *p*-toluenesulfonamide groups in probes **4** and **5**. However, in the excited state dansyl moiety of dyads **1** and **2** binds with two more Cu^{2+} ions to form M_2L and M_3L species. In excited state, the coordination of dimethylamino group of dansyl unit with Cu^{2+} causes quenching of fluorescence between 520-600 nm due to dansyl moiety and also restricts the photoinduced electron transfer from dimethylamino to anthracene moiety to release its fluorescence between 450–510 nm. This simultaneous quenching and release of fluorescence respectively due to dansyl and anthracene moieties emulates into Cu^{2+} induced ratiometric change (Scheme 2). The optimisation of structures for dyads **1** and **2** at B3LYP/6-31G level shows average distance 6–7 Å between two fluorophores (Fig. S13, ESI†) and is sufficiently small for communication between two fluorophores. Therefore, in comparison to earlier reported single fluorophore based pyrenylmethylsulfonamide probe where the ratiometric estimation of

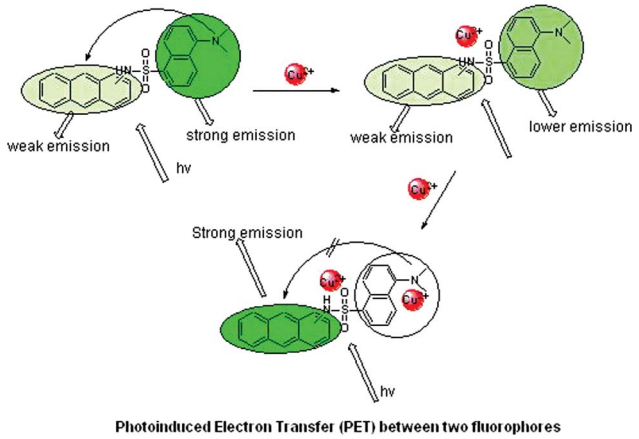

Scheme 2 Proposed mechanism for fluorescence enhancement.

Cu^{2+} became effective due to conversion of monomer emission in free probe to excimer emission in case of its Cu^{2+} complex, but in the present case the variation in communication between two fluorophores (anthracene and dansyl moieties) enables the ratiometric evaluation of Cu^{2+} through Cu^{2+} mediated restriction of PET from dansyl moiety to anthracene moiety.

Conclusions

Dyads **1** and **2** in the ground state interact with only one Cu^{2+} to generate ICT induced color changes. In excited state, the coordination of dimethylamino group of dansyl unit with Cu^{2+} causes quenching of fluorescence due to dansyl moiety and also restricts the photoinduced electron transfer from dimethylamino to anthracene moiety to release its fluorescence. This simultaneous quenching and release of fluorescence respectively due to dansyl and anthracene moieties allows ratiometric estimation of Cu^{2+} ions (1–50 μM) in CH_3CN–H_2O (7 : 3) under physiological condition.

Experimental

General comments

Melting points were determined in open capillaries and are uncorrected. JEOL A1 spectrometer was used for recording ^1H NMR spectra at 300 MHz and ^{13}C NMR spectra at 75 MHz. All chemical shifts are reported in ppm relative to the TMS as an internal reference. The assignments of the NMR signals were carried out under using decoupling experiments and ^1H-^1H COSY. UV-Vis spectroscopy analysis was carried out on a Shimadzu UV-2450 PC UV-Vis Spectrophotometer by using slit widths of 1.0 nm and matched quartz cells. Fluorescence spectra were measured on a Varian Cary Eclipse fluorescence spectrophotometer. For measurements in CH_3CN : H_2O (7 : 3) at pH 7.0 ± 0.1 (10 mM HEPES buffer), the fluorescence titrations were carried out in measuring flasks as the complete change was not instantaneous. The prepared solutions were kept for 8–12 h before recording their fluorescence spectra and showed enhanced accuracy. All absorption and fluorescence scans were saved as ACS II files and further processed in Excel™ to produce all graphs shown. Spectral data has been evaluated using Specfit 32

analysis to get the formation constants and the species distribution diagrams.

General procedure for synthesis of dyads 1–5

To the stirred solution of 1-anthracenamine (**7**) (293 mg, 1 mmol) and Et_3N (1 mmol) in dry CH_2Cl_2 (20 ml) at RT, the solution of dansyl chloride (**6**) (324 mg, 1.2 mmol) in dry CH_2Cl_2 (10 ml) was added during 5 min and stirring of the reaction mixture was continued for 8 h. The reaction mixture was washed with water, the solvent was removed under vacuum and the residue was column chromatographed on silica gel and was recrystallized from CH_2Cl_2 to get pure 5-dimethylamino-naphthalene-1-sulfonic acid anthracen-1-yl-amide (**1**). Similarly reaction of 2-anthracenamine (**8**)/aniline (**9**) with dansyl chloride (**6**) gave dyad **2**/**3**. And the reaction of (**7**) and (**8**) with *p*-toluenesulfonyl chloride (**10**) gave (**4**) and (**5**), respectively.

Dyad 1. (65%) as a yellow solid, mp 220 °C (from CH_2Cl_2), δ_H (300 MHz; $CDCl_3$; Me_4Si) 2.76 (6 H, s, $N(CH_3)_2$), 7.09 (1 H, br s, NH exchanges with D_2O), 7.23 (1 H, t, *J* 7.8, ArH), 7.28–7.44 (6 H, m, ArH), 7.67 (1 H, t, *J* 7.5, Dan-*H*), 7.79–7.87 (2 H, m, ArH), 7.99 (1 H, s, ArH), 8.02 (1 H, d, *J* 6.0, ArH), 8.28 (1 H, s, Dan-*H*), 8.33 (1 H, d, *J* 8.1, ArH), 8.63 (1 H, d, *J* 8.1, ArH); δ_C (75.5 MHz; $CDCl_3$; Me_4Si) 45.29, 115.23, 118.70, 120.38, 123.03, 123.28, 124.55, 125.61, 125.83, 126.71, 127.66, 127.75, 128.36, 128.61, 129.98, 130.20, 130.68, 131.48, 131.91, 134.39, 152.18; HRMS (ESI) found 449.1300 (M+Na), calcd for $C_{26}H_{22}N_2O_2S$+Na 449.1302

Dyad 2. (65%) as a yellow solid, mp 178 °C (from CH_2Cl_2), δ_H (300 MHz; $CDCl_3$; Me_4Si) 2.85 (6 H, s, $N(CH_3)_2$), 6.92 (1H, br s, NH exchanges with D_2O), 7.05 (1 H, dd, $J_{1,2}$ 9.0, $J_{1,3}$ 1.8, AnthH-3), 7.19 (1 H, d, *J* 7.2, Dan-*H6*), 7.36–7.46 (3 H, m, AnthH-6,7, Dan-*H*3), 7.52 (1 H, d, $J_{1,3}$ 1.8, AnthH-1), 7.61 (1 H, dd, *J* 8.4 and 7.5, Dan-*H7*), 7.78 (1 H, d, *J* 9.0, AnthH-4), 7.91(1 H, d, *J* 9.1, AnthH-5/8), 7.93 (1 H, d, *J* 9.0, AnthH-5/8), 8.18 (1 H, s, AnthH-9/10), 8.23 (1 H, dd, $J_{1,2}$ 7.5 and $J_{1,3}$ 1.2, DanH-4), 8.27 (1 H, s, AnthH-9/10), 8.40 (1 H, d, *J* 9.0, DanH-8), 8.45 (1 H, d, *J* 8.4, DanH-2/4); δ_C (75.5 MHz; $CDCl_3$; Me_4Si) 45.34, 115.23, 117.26, 118.38, 121.20, 123.09, 125.25, 125.55, 125.72, 126.08, 127.79, 128.08, 128.72, 129.22, 129.65, 129.79, 130.41, 130.94, 131.21, 131.27, 131.99, 133.29, 134.03; HRMS (ESI) found 449.1300 (M+Na), calcd for $C_{26}H_{22}N_2O_2S$+Na 449.1302.

Probe 3. (85%) as a yellow solid, mp 135 °C (from CH_2Cl_2), δ_H (300 MHz; $CDCl_3$; Me_4Si) 2.87 (6 H, s, $N(CH_3)_2$), 6.67 (1 H, br s, NH exchanges with D_2O), 6.89 (2 H, m, ArH), 7.02–7.19 (4 H, m, ArH), 7.42 (1 H, t, *J* 7.5, ArH), 7.58 (1 H, t, *J* 8.1, ArH), 8.15 (1 H, d, *J* 7.2, ArH), 8.32 (1 H, d, *J* 8.7, ArH), 8.49 (1 H, d, *J* 8.4, ArH); δ_C (75.5 MHz; $CDCl_3$; Me_4Si) 45.38, 115.20, 118.42, 121.62, 123.07, 125.27, 128.60, 129.12, 129.61, 129.79, 130.33, 130.81, 134.08, 136.39, 152.09. HRMS (ESI) found 349.0987 (M+Na); calcd for $C_{18}H_{18}N_2O_2S$+Na 349.0989.

Probe 4. (70%) as a yellow solid, mp 200 °C (from CH_2Cl_2), δ_H (300 MHz; $CDCl_3$; Me_4Si) 2.28 (3 H, s, CH_3), 6.88 (1 H, br s, NH exchanges with D_2O), 7.14 (2 H, d, *J* 8.1, ArH), 7.31–7.38 (2 H, m, ArH), 7.46–7.49 (2 H, m, ArH), 7.68 (2 H, d, *J* 8.1, ArH), 7.86–7.98 (3 H, m, ArH), 8.29 (1 H, s, ArH), 8.39 (1 H, s, ArH); δ_C (75.5 MHz; $CDCl_3$; Me_4Si) 21.41, 120.34, 121.70, 124.60, 125.91, 126.01, 127.0, 127.22, 127.37, 127.46, 127.82, 128.45, 129.56, 131.35, 131.65, 131.74, 132.11, 136.47, 143.86. HRMS (ESI) found 370.0878 (M+Na); calcd for $C_{21}H_{17}NO_2S$+Na 370.0880.

Probe 5. (75%) as a light yellow solid, mp 175 °C (from CH_2Cl_2), δ_H (300 MHz; $CDCl_3$; Me_4Si) 2.33 (3 H, s, CH_3), 6.75 (1 H, br s, NH exchanges with D_2O), 7.18–7.23 (3 H, m, ArH), 7.45 (2 H, quintet, ArH), 7.65 (1 H, s, ArH), 7.70 (2 H,d, *J* 8.4, ArH), 7.87–7.97 (3 H, m, ArH), 8.28 (1 H, s, ArH), 8.34 (1 H, s, ArH); δ_C (75.5 MHz; $CDCl_3$; Me_4Si) 21.47, 117.21, 121.29, 125.33, 125.63, 125.81, 126.20, 127.27, 127.84, 128.14, 129.33, 129.69, 129.85, 131.32, 131.43, 132.11, 133.46, 135.98, 143.98. HRMS (ESI) found 370.0878 (M+Na); calcd for $C_{21}H_{17}NO_2S$+Na 370.0880.

Acknowledgements

We thank DST, New Delhi, for Rammana fellowship to SK and FIST programme and IISc Bangalore for HRMS.

References

1 (*a*) L. Fabrizzi and A. Poggi, *Chem. Soc. Rev.*, 1995, **24**, 197–202; (*b*) A. P. de Silva, H. Q. N. Gunaratne, T. Gunnlaugsson, A. J. M. Huxley, C. P. McCoy, J. T. Rademacher and T. E. Rice, *Chem. Rev.*, 1997, **97**, 1515–1566; (*c*) L. Prodi, F. Bolletta, M. Montalti and N. Zaccheroni, *Coord. Chem. Rev.*, 2000, **205**, 59–83; (*d*) B. Valeur and I. Leray, *Coord. Chem. Rev.*, 2000, **205**, 3–40; (*e*) A. P. de Silva, D. B. Fox, A. J. M. Huxley and T. S. Moody, *Coord. Chem. Rev.*, 2000, **205**, 41–57.

2 *Fluorescent Chemosensors for Ion and Molecule Recognition*, ed. J. P. Desvergne and A. W. Czarnik, Kluwer Academic Publishers: Dordrecht, The Netherlands, 1997.

3 (*a*) D. Strausak, J. F. B. Mercer, H. H. Dieter, W. Stremmel and G. Multhaup, *Brain Res. Bull.*, 2001, **55**, 175; (*b*) B. Sarkar, *In Metal Ions in Biological Systems*, H. Siegel, A. Siegel, ed.; Marcel Dekker: New York, 1981; Vol. 12, p 233.

4 E. L. Que, D. W. Domaille and C. J. Chang, *Chem. Rev.*, 2008, **108**, 1517–1549.

5 Turn-off fluorescent sensors for Cu^{2+}: (*a*) W. Wang, A. Fu, J. You, G. Gao, J. Lan and L. Chen, *Tetrahedron*, 2010, **66**, 3695–3701; (*b*) S. Seo, H. Y. Lee, M. Park, J. M. Lim, D. Kang, J. Yoon and J. H. Jung, *Eur. J. Inorg. Chem.*, 2010, 843–847; (*c*) J. Zheng, C. Xiao, Q. Fei, M. Li, B. Wang, G. Feng, H. Yu, Y. Huan and Z. Song, *Nanotechnology*, 2010, **21**, 045501; (*d*) H. H. Wang, L. Xue, Z. J. Fang, G. P. Li and H. Jiang, *New J. Chem.*, 2010, **34**, 1239–1242; (*e*) X. H. Zhao, Q. J. Ma, X. B. Zhang, B. Huang, Q. Jiang, J. Zhang, G. L. Shen and R. Q. Yu, *Anal. Sci.*, 2010, **26**, 585–590; (*f*) P. Comba, R. Kramer, A. Mokhir, K. Naing and E. Schatz, *Eur. J. Inorg. Chem.*, 2006, 4442–4448; (*g*) Y. J. Lee, D. Seo, J. Y. Kwon, G. Son, M. S. Park, Y. H. Choi, J. H. Soh, H. N. Lee, K. D. Lee and J. Yoon, *Tetrahedron*, 2006, **62**, 12340–12344; (*h*) J. P. Sumner, N. M. Westerberg, A. K. Stoddard, T. K. Hurst, M. Cramer, R. B. Thompson, C. A. Fierke and R. Kopelman, *Biosens. Bioelectron.*, 2006, **21**, 1302–1308.

6 Turn-on fluorescent sensors for Cu^{2+}: (*a*) R. Martinez, A. Espinosa, A. Tarraga and P. Molina, *Tetrahedron*, 2010, **66**, 3662–3667; (*b*) M. H. Kim, H. H. Jang, S. Yi, S. Chang and M. S. Han, *Chem. Commun.*, 2009, 4838–4840; (*c*) Z. Xu, J. Yoon and D. R. Spring, *Chem. Commun.*, 2010, **46**, 2563–2565; (*d*) X. Chen, M. Jou, H. Lee, S. Kou, J. Lim, S. W. Nam, S. Park, K. M. Kim and J Yoon, *Sens. Actuators, B*, 2009, **137**, 597–602; (*e*) K. W. K. Swamy, S. K. Ko, S. Kwon, H. Lee, C. Mao, J. M. Kim, K. H. Lee, J. Kim, I. Shin and J. Yoon, *Chem. Commun.*, 2008, 5915–5917; (*f*) J. Liu and Y. Lu, *J. Am. Chem. Soc.*, 2007, **129**, 9838–9839; (*g*) Y. Xiang, A. Tong, P. Jin and Y. Ju, *Org. Lett.*, 2006, **8**, 2863–2866; (*h*) Z. C. Wen, R. Yang, H. He and Y. B. Jiang, *Chem. Commun.*, 2006, 106–108.

7 Ratiometric fluorescent sensors for Cu^{2+}: (*a*) M. Liu, H. Zhao, X. Quan, S. Chen and H. Yu, *Chem. Commun.*, 2010, **46**, 1144–1146; (*b*) M. Royzen, Z. Dai and J. W. Canary, *J. Am. Chem. Soc.*, 2005, **127**, 1612–1613; (*c*) D. W. Domaille, L. Zeng and C. J. Chang, *J. Am. Chem. Soc.*, 2010, **132**, 1194–1195; (*d*) S. Goswami, D. Sen and N. K. Das, *Org.*

Lett., 2010, **12**, 856–859; (*e*) Z. Xu, J. Pan, D. R. Spring, J. Cui and J. Yoon, *Tetrahedron*, 2010, **66**, 1678–1683; (*f*) Y. Zhou, F. Wang, Y. Kim, S. J. Kim and J. Yoon, *Org. Lett.*, 2009, **11**, 4442–4445; (*g*) W. Lin, L. Yuan, W. Tan, J. Feng and L. Long, *Chem.–Eur. J.*, 2009, **15**, 1030–1035; (*h*) N. Shao, J. Y. Jin, H. Wang, Y. Zhang, R. H. Yang and W. H. Chan, *Anal. Chem.*, 2008, **80**, 3466–3475; (*i*) H. J. Kim, J. Hong, A. Hong, S. Ham, J. H. Lee and J. S. Kim, *Org. Lett.*, 2008, **10**, 1963–1966; (*j*) R. Martinez, A. Espinosa, A. Tarraga and P. Molina, *Tetrahedron*, 2008, **64**, 2184–2191; (*k*) Z. Xu, X. Qian and J. Cui, *Org. Lett.*, 2005, **7**, 3029–3032.

8 (*a*) Z. Zhou, M. Yu, H. Yang, K. Huang, F. Li, T. Yi and C. Huang, *Chem. Commun.*, 2008, 3387–3389; (*b*) V. S. Jisha, A. J. Thomas and D. Ramaiah, *J. Org. Chem.*, 2009, **74**, 6667–6673; (*c*) M. Frigoli, K. Ouadahi and C. Larpent, *Chem.–Eur. J.*, 2009, **15**, 8319–8330; (*d*) N. Singh, N. Kaur, B. McCaughan and J. F. Callan, *Tetrahedron Lett.*, 2010, **51**, 3385–3387.

9 (*a*) C. R. Lohani and K. H. Lee, *Sens. Actuators, B*, 2010, **143**, 649–654; (*b*) S. V. Bhosale, S. V. Bhosale, M. B. Kalyankar and S. J. Langford, *Org. Lett.*, 2009, **11**, 5418–5421; (*c*) N. Singh, N. Kaur, J. Dunn, M. MacKay and J. F. Callan, *Tetrahedron Lett.*, 2009, **50**, 953–956; (*d*) F. Qu, J. Liu, H. Yan, L. Peng and H. Li, *Tetrahedron Lett.*, 2008, **49**, 7438–7441.

10 (*a*) Dansyl based probes: H. W. Li, Y. Li, Y. Q. Dang, L. J. Ma, Y. Wu, J. Hou and L. Wu, *Chem. Commun.*, 2009, 4453–4455; (*b*) N. Zhang, Y. Chen, M. Yu and Y. Liu, *Chem.–Asian J.*, 2009, **4**, 1697–1702; (*c*) J. Yin, X. Guan, D. Wang and S. Liu, *Langmuir*, 2009, **25**, 11367–11374; (*d*) R. Peng, F. Wang and Y. Sha, *Molecules*, 2007, **12**, 1191–1201; (*e*) M. H. Al-Sayah and T. M. El-Chami, *Supramol. Chem.*, 2009, **21**, 650–657; (*f*) M. H. Lee, H. J. Kim, S. Yoon, N. park and J. S. Kim, *Org. Lett.*, 2008, **10**, 213–216; (*g*) M. Suresh, S. Mishra, S. K. Mishra, E. Suresh, A. K. Mandal, A. Shrivastav and A. Das, *Org. Lett.*, 2009, **11**, 2740–2743.

